Advanced Parametric Modelling of Pyramidal Trusses

Jackson S. Rocha Segundo[1], Ricardo A. M. Silveira[1], Rafael C. Barros[2], Dalilah Pires[3], Ígor J. M. Lemes[4]

[1]*Dept. of Civil Engineering, Federal University of Ouro Preto*
Morro do Cruzeiro, 35400-000, Ouro Preto/MG, Brazil
jackson.segundo@aluno.ufop.edu.br, ricardo@ufop.edu.br
[2]*Sereng Engineering & Consulting*
34006-056, Nova Lima, Minas Gerais, Brazil
rafaelcesario@hotmail.com
[3]*Dept. de Tecnologia em Engenharia Civil, Computação, Automação, Telemática e Humanidades (DTECH), Universidade Federal de São João Del-Rei*
Campus Alto do Paraopeba, Rod. MG 443, KM 7, 36420-000 Ouro Branco/MG, Brazil
dalilah@ufsj.edu.br
[4]*Department of Engineering, Federal University of Lavras*
Campus Universitário Kennedy, 37200-000, Lavras/MG, Brazil
igor.lemes@ufla.br

Abstract. Trusses are an affordable and easy solution for engineers, especially when spanning large distances. It is notorious that several aspects of trusses influence their behavior. By accounting for material and geometric non-linearities, this study examines the behavior of pyramid trusses under vertical load. Practical applications make these structures valuable as either a primary or secondary component. This study looks at how elastic and inelastic stability of pyramidal trusses are influenced by factors like focus height, base radius and number of bars. Therefore, it will be possible to identify the ideal stability and strength configurations for pyramidal trusses. The advanced nonlinear analyzes intend to use results from the literature or obtained via other softwares in the calibration of the proposed numerical models. It will be possible to perceive under what conditions the pyramidal truss presents gain and loss of rigidity, indicating alternatives for designers that envisage such structure shape.

Keywords: pyramidal trusses, advanced analysis, material and geometric non-linearities, stability and strength.

1 Introduction

Designers around the world have trusses as great allies in structural projects, because this system is an excellent solution in terms of resistance, practicality and economy. Therefore, they are widely used in various engineering situations, with emphasis on roofs, and have the advantageous characteristic of facing large spans and an excellent load/weight ratio. Due to their extensive use in civil construction, both as main or secondary components, pyramidal trusses have an immediate and growing interest. Such structures generally exhibit strongly non-linear behavior and are susceptible to catastrophic buckling. Such structures are the spatial counterpart of the classic von Mises truss.

Several researchers in recent years have studied the pyramidal trusses behavior. Ligarò and Valvo [1] proposed an analytical expression of the internal energy considering moderate elastic deformations; Orlando *et al*. [2] derived the dynamic nonlinear equations for such trusses under vertical harmonic loading; and Santana *et al*. [3, 4] studied the load capacity and stability of these systems, as well as the transient nonlinear behavior.

This paper aims to study the parameters that influence the second-order elastic and inelastic behavior of pyramidal trusses. The goal is to assess the ideal design conditions for such structures. In the following sections are detailed the truss geometric nonlinear formulation and the elastoplastic constitutive model adopted. The numerical results obtained are presented in sequence and allow drawing interesting conclusions about these structural systems.

2 Finite element formulation and constitutive law

Structural engineering problems can present several sources of non-linearity: geometric, material, connections, boundary, etc. Considering such nonlinearity means bringing the structural model problem closer to the structural real problem.

Consider the truss element showed in Fig. 1 and that it has constant cross-section area A. The bar coordinates, (X_1, Y_1, Z_1) and (X_2, Y_2, Z_2), represent the initial configuration of the element, also referred to as reference coordinates. After the displacements, the bar has a new configuration described by the coordinates (x_1, y_1, z_1) and (x_2, y_2, z_2), as presented in Fig. 1. The initial length L_0, also known as the reference, and the current length L are calculated by:

$$L_0 = \sqrt{X_2 - X_1 \ + \ Y_2 - Y_1 \ + \ Z_2 - Z_1} \text{ and } L = \sqrt{x_2 - x_1 \ + \ y_2 - y_1 \ + \ z_2 - z_1}\,. \tag{1}$$

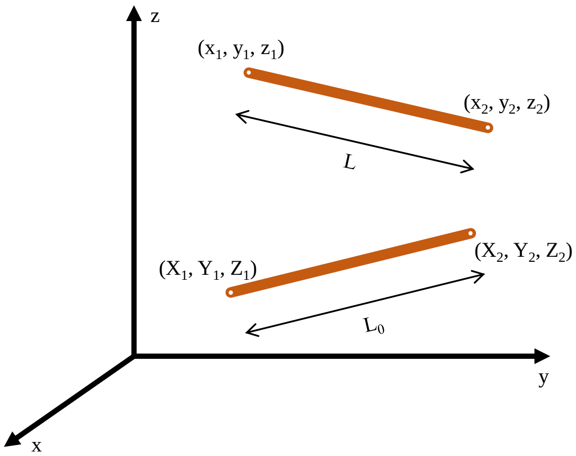

Figure 1. Positional truss element

The element tangent stiffness matrix $\boldsymbol{K}$ and the internal force vector $\boldsymbol{F}$ are obtained according to the equations [5]:

$$\boldsymbol{K} = \boldsymbol{K}_e + \boldsymbol{K}_g = \frac{EA}{L_0^3}\boldsymbol{B} + \frac{EA\varepsilon_G}{L_0}\boldsymbol{C} \quad \text{and} \quad \boldsymbol{F} = \frac{EA\varepsilon_G}{L_0}\boldsymbol{m} \tag{2}$$

in which:

$$\boldsymbol{B} = \boldsymbol{r}\boldsymbol{r}^T; \boldsymbol{C} = \begin{bmatrix} \boldsymbol{I}_3 & -\boldsymbol{I}_3 \\ -\boldsymbol{I}_3 & \boldsymbol{I}_3 \end{bmatrix}; \boldsymbol{r}^T = \begin{bmatrix} x_1 - x_2, & y_1 - y_2, & z_1 - z_2, & x_2 - x_1, & y_2 - y_1, & z_2 - z_1 \end{bmatrix} \tag{3}$$

and ε_G is the Green-Lagrange strain given by:

$$\varepsilon_G = \frac{L^2 - L_0^2}{2L_0^2}. \tag{4}$$

The material non-linear behavior is very recurrent in structural engineering problems and can leads, in some situations, to phenomena such as plastification, damage, fracturing, cracking, etc. The inclusion of such non-linear effect increases the problem modelling complexity and the faithfully representing the material behavior subjected to any request is a difficult task. Thus, it is common to approximate the material non-linear behavior in an idealized way.

In elastoplastic constitutive models, it is considered that after reaching the yield stress, any load increase will cause irreversible plastic deformations to the body. Bathe [6] clarifies that three properties are necessary to characterize the material and calculate the plastic deformations: the flow function; the flow rule; and the hardening rule that determines how the yield function is modified during the plastic regime. Yaw [7] points out that such models are widely used to simulate the behavior of materials that exhibit hardening after yielding, as occurs in metals, and of materials that exhibit softening after maximum load, as reported by Chen and Han [8].

In the present paper, the works of Simo and Hughes [9] and Yaw [7] were used for the implemented elastoplastic model, as in Souza *et al*. [10]. The total specific strain (ε) is divided into two parts, the elastic strain (ε_e) and the plastic strain (ε_p), as given below:

$$\varepsilon = \varepsilon_e + \varepsilon_p. \tag{5}$$

With this, the value of the stress σ is:

$$\sigma = E_0 \varepsilon_e = E_0 \left(\varepsilon - \varepsilon_p \right) \tag{6}$$

where E_0 is the initial modulus of elasticity. Therefore, the flow criterion that is a function of the stress is expressed by:

$$f\left(\sigma\right) = \left|\sigma\right| - G\left(\alpha\right) \tag{7}$$

where $G(\alpha)$ is a function describing the variation of the yield stress σ_y which, for linear hardening, is given by:

$$G\left(\alpha\right) = \sigma_y - B\alpha \tag{8}$$

where α is the hardening parameter and B is the plastic modulus. In the equation above, the positive value of B characterizes the hardening of the material. If this value is negative, it indicates a softening. The null value, in turn, indicates the perfect elastoplastic model. For linear hardening, the elastoplastic tangent modulus of elasticity is given by:

$$E = \frac{E_0 B}{E_0 + B}. \tag{9}$$

3 Methodology for solving nonlinear structural problem

As performed on this work, the nonlinear truss problem is solved through an incremental-iterative procedure [11], which is characterized by two distinct phases: the first, predicted phase; and the second, corrective phase. The first involves the solution of the incremental displacements, obtained from a load increment. The second phase aims to correct the incremental internal forces and obtain the system equilibrium.

In FEM context, the nonlinear equilibrium equation can be written as:

$$\boldsymbol{F}_i\left(\boldsymbol{U}, \boldsymbol{P}\right) = \lambda \boldsymbol{F}_r \tag{10}$$

in which $\boldsymbol{F}_i$ and $\boldsymbol{F}_r$ are the internal and external forces vectors, respectively. If large displacements and second-order effects are considered, $\boldsymbol{F}_i$ is dependent of the nodal displacements $\boldsymbol{U}$ and the internal forces $\boldsymbol{P}$. The external force vector $\boldsymbol{F}_r$ is scaled through the load parameter λ and only its direction matters.

Before describing the numerical procedures adopted in obtaining the problem equilibrium for a given load increment, to facilitate understanding, considerations are made regarding the notation used, that is:

- It is considered that the displacement field and the stress state of the structure in the previous load step (t) are known, and it is desired to determine the equilibrium configuration for the current load step ($t + \Delta t$);
- k is the counter for the number of iterations. The predicted solution occurs for $k = 0$ and the iteration cycle for values of $k \neq 0$;
- λ and $\boldsymbol{U}$ are the total load parameter and nodal displacement vector, respectively;
- $\Delta\lambda$ and $\Delta\boldsymbol{U}$ are the incremental load parameter and nodal displacement vector, respectively, determined from the last equilibrium configuration;
- $\delta\lambda$ and $\delta\boldsymbol{U}$ are the load parameter and nodal displacement vector corrections during the iterative process.

3.1 Predicted solution

The first step to obtain the initial tangent incremental solution ($\Delta\lambda^0$ and $\Delta\boldsymbol{U}^0$) consists of assembling, using information from the last structural equilibrium configuration, the tangent stiffness matrix, $\boldsymbol{K}$. Next, the tangential nodal displacement vector $\delta\boldsymbol{U}_r$ is obtained according to:

$$\boldsymbol{K}\delta\boldsymbol{U}_r = \boldsymbol{F}_r. \tag{11}$$

The automatic selection of the initial increment of the load parameter can be done through a load increment strategy [12]. After defining the initial load increment, $\Delta\lambda^0$, the incremental nodal displacement vector, $\Delta\boldsymbol{U}^0$, is determined by:

$$\Delta\boldsymbol{U}^0 = \Delta\lambda^0\delta\boldsymbol{U}_r. \tag{12}$$

Then, the total load parameter and nodal displacement vector are updated:

$$^{t+\Delta t}\lambda = {}^{t}\lambda + \Delta\lambda^0\text{; and } {}^{t+\Delta t}\boldsymbol{U} = {}^{t}\boldsymbol{U} + \Delta\boldsymbol{U}^0 \tag{13}$$

where $^{t}\lambda$ and $^{t}\boldsymbol{U}$ characterize the system equilibrium point in the last load step t.

The solutions defined by eqs. (13) normally do not satisfy the equilibrium conditions. Therefore, a cycle of iterations is necessary to obtain the system equilibrium.

3.2 Iterative cycle

The Newton-Raphson Method (NRM) aims to determine the roots of a nonlinear equations system. In the structural problem context, the equation whose roots need to be determined is given by eq. (10). In its default scheme, NRM corrects only the nodal displacement vector, $\boldsymbol{U}$, during the iterative cycle. The load parameter, λ, remains unchanged during this process. This procedure limits the solution up to the first load limit point. If the objective is to obtain the complete equilibrium path, it is necessary to allow the change of the load parameter during the iterative cycle.

The problem then consists of establishing a series of corrections for a given initial estimate of the root until a satisfactory value within the required precision is obtained [13]. By following the general technique proposed by Batoz and Dhatt [14], one can consider a change in the nodal displacement vector governed by the following equilibrium equation:

$$\boldsymbol{K}^{(k-1)}\delta\boldsymbol{U}^k = \boldsymbol{g}\left(\boldsymbol{U}^{(k-1)},\lambda^k\right) \tag{14}$$

in which $\boldsymbol{g}$ represents the unbalanced force vector (or gradient) that must be nullified during the interactive cycle. This vector is a function of the total nodal displacements $\boldsymbol{U}$, calculated in the last iteration (k-1), and of the load parameter, λ, in the current iteration (k), which becomes an unknown of the problem, that is:

$$\lambda^k = \lambda^{(k-1)} + \delta\lambda^k \tag{15}$$

where $\delta\lambda^k$ is the load parameter correction. Substituting Eq. (15) into (14), we get:

$$\boldsymbol{K}^{(k-1)}\delta\boldsymbol{U}^k = -\left[\boldsymbol{F}_i^{(k-1)} - \left(\lambda^{(k-1)} + \delta\lambda^k\right)\boldsymbol{F}_r\right]. \tag{16}$$

The above equation can be rewritten as follows:

$$\boldsymbol{K}^{(k-1)}\delta\boldsymbol{U}^k = -\boldsymbol{g}^{(k-1)} + \delta\lambda^k\boldsymbol{F}_r \tag{17}$$

this being the form to be worked on during the iterative cycle.

The nodal displacement vector correction can be divided into two parts:

$$\delta\boldsymbol{U}^k = \delta\boldsymbol{U}_g^k + \delta\lambda^k\delta\boldsymbol{U}_r^k \tag{18}$$

with:

$$\delta\boldsymbol{U}_g^k = \left(\boldsymbol{K}^{(k-1)}\right)^{-1}\boldsymbol{g}^{(k-1)} \text{ and } \delta\boldsymbol{U}_r^k = \left(\boldsymbol{K}^{(k-1)}\right)^{-1}\boldsymbol{F}_r \tag{19}$$

in which $\delta\boldsymbol{U}_g$ is the vector correction that is obtained with the conventional NRM, without changing the load parameter; $\delta\boldsymbol{U}_r$ is the iterative displacement vector resulting from the application of $\boldsymbol{F}_r$.

The only unknown in eq. (18) is the load parameter $\delta\lambda^k$ correction, which is determined from some iteration strategy [12]. Once the iterative solution, $\delta\lambda^k$, and $\delta\boldsymbol{U}^k$, is obtained, the incremental and total variables of the problem are updated. The process is interrupted, indicating a new position of equilibrium, when convergence criteria are satisfied. The criterion is based on force relations, calculated at the beginning of the current iteration using data from the previous iteration, is used here [12].

4 Numerical examples

Considering second-order and elastoplastic effects, it is analysed now the pyramid truss previously studied by Hrinda [15] and presented in Fig. 2. The influence of the focus height, material modulus of elasticity, distance between the center node and the end node, and the number of bars is investigated. The data used by Hrinda [15] served as reference for various evaluated parameters. For the elastoplastic analysis, the results obtained via Mastan2 software [16] were used.

This pyramidal system has eight members and 500 inches long in the xy plane. The central out-of-plane nodal point has a height of 40 in; the modulus of elasticity is equal to 10000 lb/in²; and the cross-section area of the bars is equal to 10 in². In the next subsections, each parameter variation results will be presented individually.

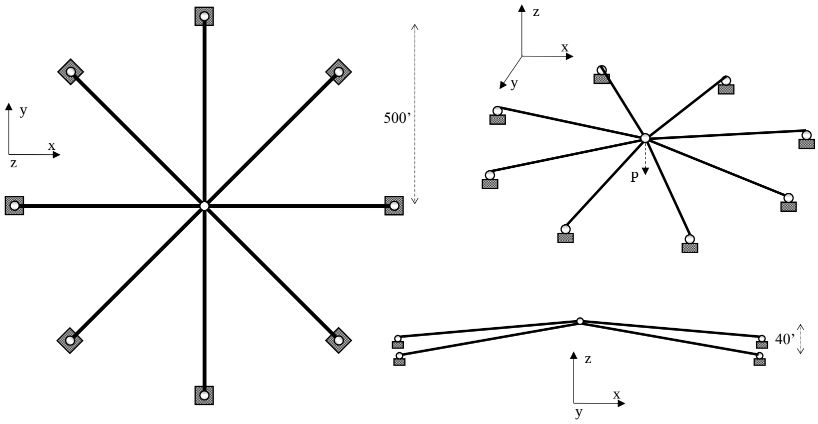

Figure 2. Original pyramidal truss [15]

4.1 Dimension of central out-of-plane node

The first parameter to be varied is the height of the out-of-plane central node. This parameter reflects the truss slump. The smaller the value, the more depressed the truss will be. Thus, evaluating this parameter provides us with information about the advantages of having a truss that is low or high and how this variable influences the general behavior of the system.

Figure 3 shows the second-order elastic responses varying the height of the out-of-plane central node. In turn, Fig. 4 shows the second-order inelastic results. It is possible to notice a good agreement with the references and the stiffness gain as the height of this dimension increases. Therefore, it is possible to state that trusses that are not very flat present greater stiffness than those that are flatter, highlighting a difference in such behavior.

4.2 Young's module

The second parameter analyzed is the material modulus of elasticity of the bars. Figures 5a and 5b present the second-order elastic and second-order elastoplastic results, respectively, and once again, see the good agreement between the answers. It is possible to notice that for smaller values of the modulus of elasticity, the material elastoplastic behavior has little relevance in the analysis. For this case, geometric nonlinear effects govern the truss behavior.

4.3 Distance in plane: center-end nodes

Another parameter analyzed is the distance between the out-of-plane central node and the end nodes. This variable represents the length of the bar projection in the xy plane. The results obtained by the present work are shown in Figs. 6a and 6b. As the previous results, good agreement with the literature is observed. As this parameter increases, a loss of truss stiffness is observed.

In the elastoplastic analyses, an interesting behavior can be noticed: for the smallest values of the radius (350 and 400), the geometric nonlinearity does not influence the structural behavior until near the second load limit point, while the influence of the physical nonlinearity is more pronounced. For intermediate values (500 and 600), it is possible to perceive the influence of the two nonlinearities on the system's behavior, pointing out that both are equally relevant to the analysis. For the highest values (800 and 1000) see that the physical non-linearity only influences the behavior of the system when the first two load limit points are exceeded, with the behavior governed until then by second-order effects.

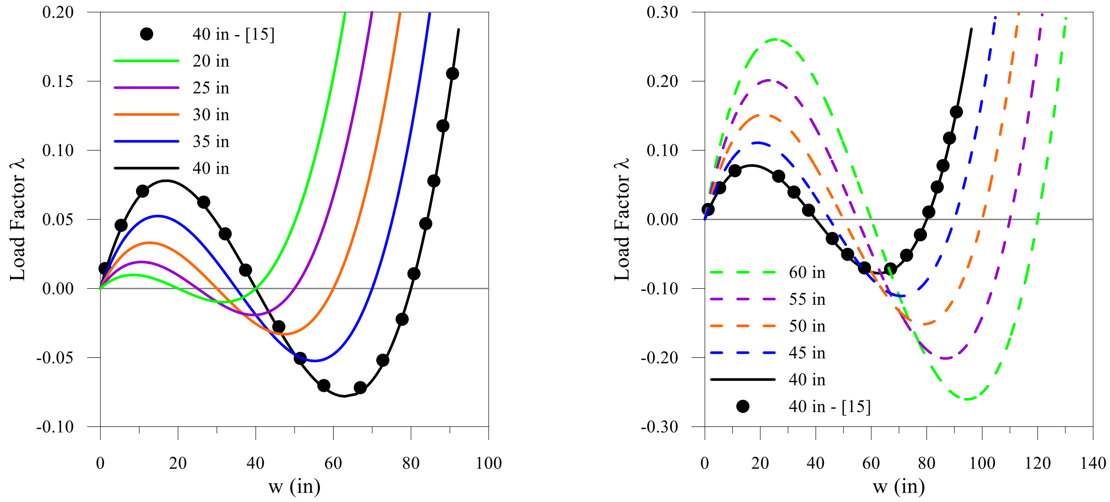

Figure 3. Pyramidal truss second-order elastic analysis of out-plane center node

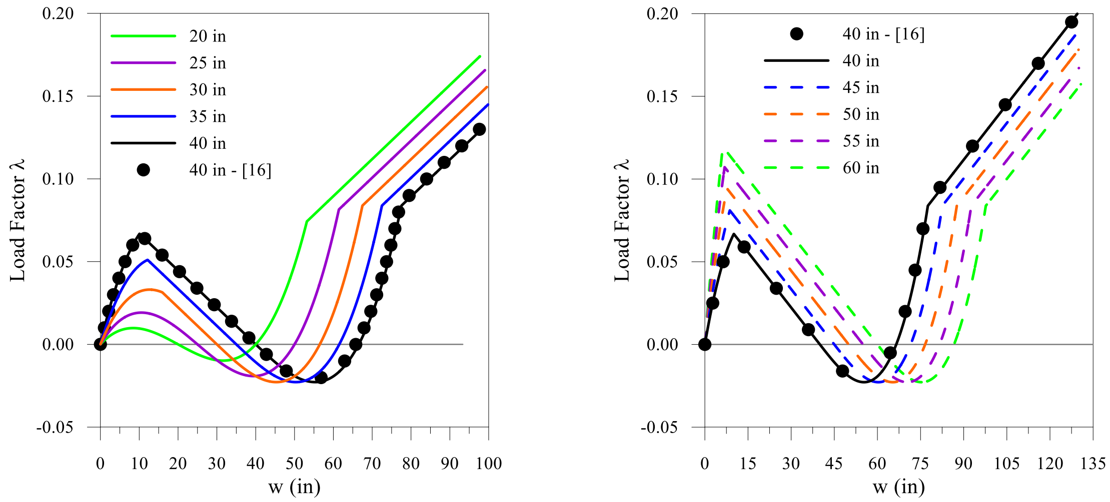

Figure 4. Pyramidal truss second-order elastoplastic analysis of out-plane center node

4.4 Number of members

The last evaluated parameter is the number of bars in the pyramidal truss. The results are shown in Figs. 7a and 7b. Observe that the increase of bars adds rigidity to the system, as the intuition indicates. In elastoplastic study, it is possible to notice that the increase in the number of bars, the physical non-linearity becomes more relevant in the analysis, especially until reaching the first limit point.

5 Conclusions

This study numerically and parametrically evaluated the behavior of pyramidal trusses, considering physical and geometric nonlinearities. It is important to point out that this present work allows evaluating how these parameters influence the spatial structural system equilibrium. The results obtained make it possible to determine the best conditions for each variable for the most appropriate conception of the structure within the needs of the designer, be they safety, economy, or functionality.

It was possible to verify, especially in analyzes that consider the two sources of non-linearity, how each parameter changes the influence of these effects on the behavior of the curves. It should be noted that when varying some parameters, the equilibrium path for some simulations presents changes in the source of nonlinearity that governs the problem. In addition, the supported load values for the elastoplastic analyzes are lower than those verified for the elastic analyses, indicating the relevance of considering this effect in a simulation that intends to get as close as possible to the real truss problem.

Finely, it should be mentioned that this work is an initial investigation of a series of studies to be carried out regarding the non-linear structural behavior of pyramidal trusses.

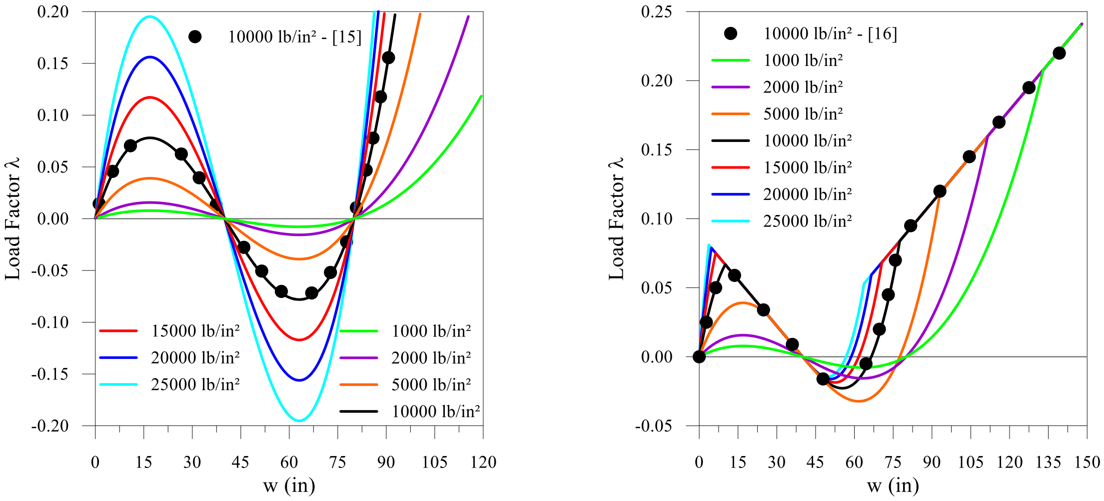

a) Elastic b) Elastoplastic

Figure 5. Pyramidal truss analysis of Young's module variation

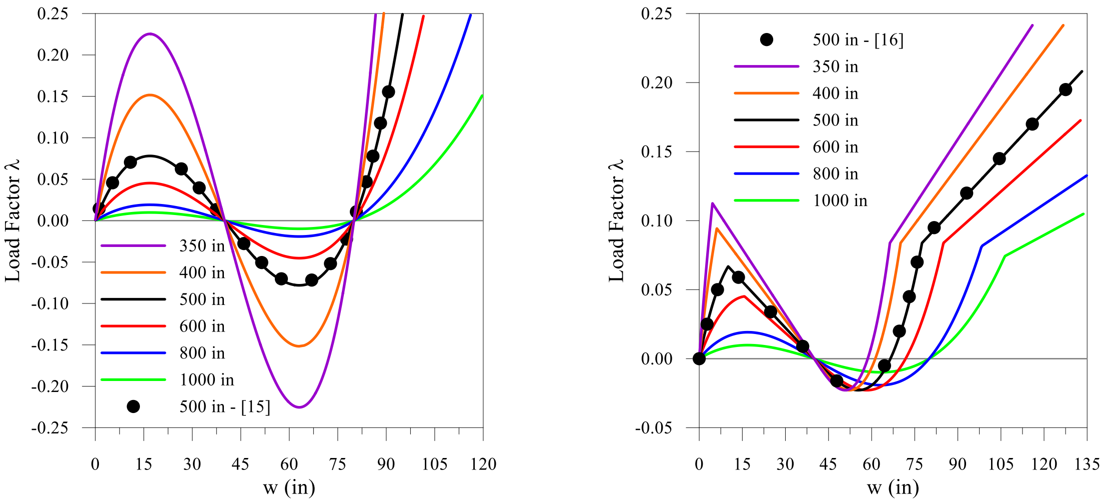

a) Elastic b) Elastoplastic

Figure 6. Pyramidal truss analysis of distance in plane: center-end nodes

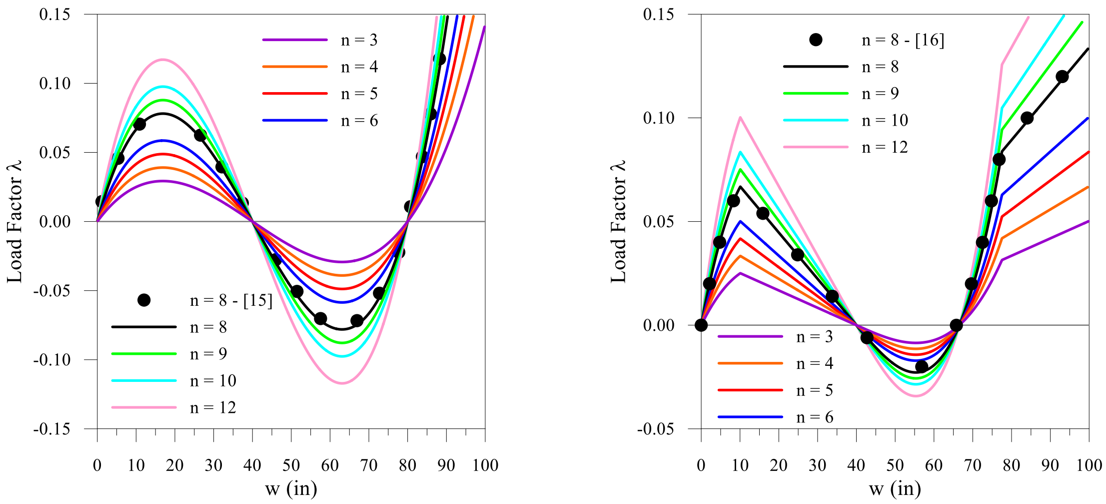

a) Elastic b) Elastoplastic

Figure 7. Pyramidal truss analysis of number of members

Acknowledgements. This work was made with the support from CAPES, CNPq, FAPEMIG, PROPEC/UFOP, PROPPI/UFOP, UFSJ and UFLA. The authors also thank the prof. Ronald Ziemian for the availability of MASTAN2.

Authorship statement. The authors hereby confirm that they are the sole liable persons responsible for the authorship of this work, and that all material that has been herein included as part of the present paper is either the property (and authorship) of the authors, or has the permission of the owners to be included here.

References

[1] S. S. Ligarò and P. S. Valvo, "Large displacement analysis of elastic pyramidal trusses". *Int. J. Solids Struct.*, vol. 43, pp. 4867-4887, 2006.

[2] D. Orlando, C. H. L. Castro and P. B. Gonçalves, "Nonlinear vibrations and instability of a bistable shallow reticulated truss". *Nonlinear Dynamics*, vol. 94, pp. 1479-1499, 2018.

[3] M. V. B. Santana, P. B. Gonçalves and R. A. M. Silveira, "Stability and load capacity of an elasto-plastic pyramidal truss". *International Journal of Solids and Structures*, vol. 171, pp. 158-173, 2019.

[4] M. V. B. Santana, P. B. Gonçalves and R. A. M. Silveira, "Nonlinear oscillations and dynamic stability of an elastoplastic pyramidal truss". *Nonlinear Dynamics*, vol. 98, pp. 2847-2877, 2019.

[5] H. B. Coda and M. Greco, "A simple FEM formulation for large deflection 2D frame analysis based on position description. *Computer Methods in Applied Mechanics and Engineering*, v.193, n. 33-35, pp. 3541-3557, 2004.

[6] K. J. Bathe. *Finite element procedures*. Prentice Hall, 2006.

[7] L. L. Yaw. *Nonlinear static – 1D Plasticity – Isotropic and Kinematic Hardening*. Walla Walla University, 2017.

[8] W. F. Chen and D. J. Han. *Plasticity for structural engineers.* J. Ross Publishing, 2007.

[9] J. Simo and T. Hughes. *Computational ineslaticity*. Springer, 2000.

[10] L. A. F. Souza, D. F. Santos and R. Y. M. Karawato, "Análise não linear física de treliças com ciclos de carregamento e descarregamento". *Revista Tecnológico*, vol. 28, n. 1, pp. 101-118, 2019.

[11] J. S. Rocha Segundo, R. A. M. Silveira, A. R. D. Silva and R. C. Barros. "Combinando as técnicas de busca linear com continuação para a solução de problemas estruturais não lineares". In: *XL Ibero-Latin American Congress on Computational Methods in Engineering (CILAMCE 2019)*, Natal, RN, pp. 1-18, 2019.

[12] A. R. D. Silva, Silva. *Sistema computacional para a análise avançada estática e dinâmica de estruturas metálicas*. Tese de Doutorado, Programa de Pós-Graduação em Engenharia Civil, Deciv/EM/UFOP, Ouro Preto-MG, Brasil, 2009.

[13] R. D. Cook, D. S. Malkus and M. E. Plesha. *Concepts and applications of finite element analysis*. Wiley, 3rd edition, 1989.

[14] J. L Batoz and G. Dhatt, "Incremental displacement algorithms for nonlinear problems*". International Journal for Numerical Methods in Engineering*, vol. 14, pp. 1262-1267, 1979.

[15] G. A. Hrinda. *Snap-through instability patterns in truss structures*. Nasa Langley Research Center, Hampton – Virginia, 2010.

[16] R. D. Ziemian and W. McGuire. MASTAN2 v.35, 2022 (http://www.mastan2.com/about.html).